HHS Public Access

Author manuscript

Cancer Res. Author manuscript; available in PMC 2017 August 15.

Published in final edited form as:

Cancer Res. 2017 February 15; 77(4): 886–896. doi:10.1158/0008-5472.CAN-16-2219.

An essential role of maspin in embryogenesis and tumor suppression

Sijana H. Dzinic[1,2], **M. Margarida Bernardo**[1,2], **Xiaohua Li**[1,2], **Rodrigo Fernandez-Valdivia**[1,2], **Ye-Shih Ho**[3], **Qing-Sheng Mi**[2,4,5], **Sudeshna Bandyopadhyay**[1,2], **Fulvio Lonardo**[1,2], **Semir Vranic**[6], **Daniel S. M. Oliveira**[1,2,7], **R. Daniel Bonfil**[1,2,7,8], **Gregory Dyson**[2,8], **Kang Chen**[2,4,7,8,9,10], **Almasa Omerovic**[1,2], **Xiujie Sheng**[11], **Xiang Han**[12], **Dinghong Wu**[4,5], **Xinling Bi**[4,5], **Dzenana Cabaravdic**[1,2], **Una Jakupovic**[1,2], **Marian Wahba**[13], **Aaron Pang**[1,2], **Deanna Harajli**[1,2], **Wael A Sakr**[1,2], and **Shijie Sheng**[1,2,8,*]

[1]Department of Pathology, Wayne State University School of Medicine (WSU, SOM), Detroit, Michigan, 48201

[2]Tumor Biology and Microenvironment Program, Barbara Ann Karmanos Cancer Institute, Detroit, MI 48201

[3]Institute of Environmental Health Sciences, WSU, SOM

[4]Department of Immunology and Microbiology, WSU, SOM

[5]Department of Dermatology, Henry Ford Health Systems, Detroit, Michigan 48201

[6]Division of Experimental Pathology, Department of Pathology, University Clinical Center, Sarajevo, Bosnia and Herzegovina

[7]Department of Urology, WSU, SOM

[8]Department of Oncology, WSU, SOM

[9]Perinatology Research Branch, Eunice Kennedy Shriver National Institute of Child Health and Human Development, National Institutes of Health (NIH), Detroit, Michigan, 48201

[10]Mucosal Immunology Studies Team, National Institute of Allergy and Infectious Diseases, NIH, Bethesda, Maryland, 20817

[11]Department of Obstetrics and Gynecology, the Third Affiliated Hospital of Guangzhou Medical University, Guangzhou, Guangdong, P.R., 510150, China

[12]Peking University Health Science Center, The 3rd Affiliated Hospital, Beijing, P.R., 100875, China

[13]Department of Internal Medicine, Sinai Grace Hospital, Detroit Medical Center, Detroit, Michigan, 48201

Abstract

[*]**Corresponding author**: Department of Pathology, Wayne State University School of Medicine, 540 East Canfield Street, Detroit, Michigan; Telephone: 313-993-8197; Fax: 313-993-4112; ssheng@med.wayne.edu.

Disclosure of Potential Conflicts of Interest: There are no potential conflicts of interest for disclosure.

Maspin (SerpinB5) is an epithelial-specific tumor suppressor gene product that displays context-dependent cellular functions. Maspin-deficient mouse models created to date have not definitively established maspin functions critical for cancer suppression. In this study, we generated a mouse strain in which exon 4 of the *Maspin* gene was deleted, confirming its essential role in development but also enabling a breeding scheme to bypass embryonic lethality. Phenotypic characterization of this viable strain established that maspin deficiency was associated with a reduction in maximum body weight and a variety of context-dependent epithelial abnormalities. Specifically, maspin-deficient mice exhibited pulmonary adenocarcinoma, myoepithelial hyperplasia of the mammary gland, hyperplasia of luminal cells of dorsolateral and anterior prostate, and atrophy of luminal cells of ventral prostate and stratum spinosum of epidermis. These cancer phenotypes were accompanied by increased inflammatory stroma. These mice also displayed the autoimmune disorder alopecia aerate. Overall, our findings defined context-specific tumor suppressor roles for maspin in a clinically relevant model to study maspin functions in cancer and other pathologies.

Keywords

tumor suppressor; Zp3-Cre recombinase; embryonic lethality; epithelial differentiation; hyperplasia; adenocarcinoma

Introduction

Maspin belongs to the serine protease inhibitor (serpin) superfamily (1). Maspin expression is epithelial-specific (2) and is predominantly confined in the nuclei of normal cells (3). Based on the X-ray crystallographic (4, 5) and phylogenetic analyses (6) maspin deviates significantly from other serpins that specifically inhibit serine proteases. We have shown that maspin cross-inhibits serine protease-like histone deacetylase 1 (HDAC1) in the nucleus (3, 7). HDAC1 primarily deacetylates histones leading to condensed chromatin and transcription repression (8, 9). Consistently, maspin commonly regulates a set of HDAC1 target genes directly involved in epithelial differentiation and cellular responses to stress or TGFβ (10).

It has been extensively reported that translocation of maspin from the nucleus to the cytoplasm or down-regulation of maspin expression correlates with worse diagnosis and stratifies with poor overall survival of cancer patients (11–15). Functional evidence demonstrates multifaceted tumor suppressive effects of maspin in limiting cancer stem cell self-renewal and plasticity, blocking cancer invasion and metastasis, and modulating cancer cell drug response (10, 16–20). While the biological evidence of the maspin effect in tumor progression was predominantly derived from *in vivo* studies using orthotropic (1, 17) and subcutaneous xenograft models (16), mouse maspin, which is 89% homologous with human maspin at the amino acid level (21), has also been shown to suppress mammary gland tumor progression in the WAP-TAg/WAP-*Maspin* bi-transgenic model (22) and IKKα-stimulated prostate tumor metastasis in the TRAMP mouse model (23). In addition, maspin protein delivered *via* non-viral liposome was shown to suppress the progression of polyoma middle T antigen-driven mammary tumor development (24). Maspin transgene expression in

TRAMP model-derived prostate tumor cells, TRAMP-C2N, blocked the tumor progression in a syngeneic xenograft model (25).

While accumulated evidence suggests that loss of maspin may directly lead to tumor development and progression, this hypothesis has to be addressed in an *in vivo* model where maspin is knocked out in a background where the effects of maspin loss in all pertinent epithelial tissues is not yet compromised by any specific oncogenic mechanism. To this end, in 2004, Gao *et al.* attempted to generate *Maspin* KO mice by targeting *Maspin* exon 7 in mouse embryonic stem cells (ESC). *Maspin* exon 7 codes for amino acids 246–375 which encompass the reactive center loop (RCL), a critical sequence necessary for the biological function of maspin (1). The resulting homozygous *Maspin*-null mice were embryonically lethal at day E 5.5 (26), whereas mice with heterozygous *Maspin* deletion were viable, but developed spontaneous prostatic intraepithelial hyperplasia in the dorsolateral lobe (27). Interestingly, a recent study by Teoh *et al.* (19) used a CMV-driven Cre-recombinase transgenic system to target *Maspin* exon 4 that codes for amino acids 103–142, encompassing the critical structures of α-helices E and F. The authors reported live birth of the resulting *Maspin* KO mice in Mendelian ratio relative to other genotypes. Teoh *et al.* analyzed tissues from two male and two female 6–8 weeks old *Maspin* KO animals and reported no abnormal development or tumor incidence. Based on these results and data from a mammary gland tumor xenograft experiment, Teoh *et al.* concluded that maspin is not required for mouse development or tumor suppression. For the field of maspin study to move forward, not only this controversy needs to be unambiguously resolved, but we also need a viable *Maspin* KO model to recapitulate the biological functions and underlying mechanisms of maspin in human diseases, especially cancer.

In the current study, we independently generated floxed *Maspin* founder mice. We showed that homozygous deletion of *Maspin* gene during oogenesis results in embryonic lethality and that lethality can be circumvented through an alternative crossbreeding scheme. Furthermore, we report the first evidence that *Maspin* deletion leads to spontaneous development of organ- and cell-type specific atrophy, hyperplasia and adenocarcinoma, signifying an essential role of maspin in tumor suppression. Taken together, the *Maspin* KO mouse model established in this study opened a new window of opportunity for fundamental studies of maspin in tumorigenesis and tumor progression and will be valuable for exploring the therapeutic potential of maspin in cancer diagnosis and treatment.

Materials and Methods

Gene targeting strategy

The floxed *Maspin* mice were generated on a C57BL/6 genetic background through commercial technical assistance by Ozgene (Perth, Australia). Briefly, the targeting construct contained loxP sites flanking exons 4 (sequence release by Vega Genome Browser as of March 2010) and a PGK-neomycin selection cassette (PGK-Neo) inserted between exons 3 and 4 (Fig. 1) The PGK-Neo cassette was also flanked by FRT sites to allow for FLPe recombinase deletion. The resulting targeting vector was transfected into the C57BL/6 Bruce 4 ESC (28) and positive clones were identified based on antibiotic resistance (29). Two selected ESC clones were injected into albino C57BL/6 blastocysts. The resulting male

chimeras were intercrossed with female albino C57BL/6 mice to obtain germline transmission. The resulting black coat offspring were screened for the targeted floxed allele by Southern blot analysis of the tail biopsy genomic DNA using the following probes: enP that binds to the + strand from 108772182–108773091; tP3 that binds to the + strand from 108781463–108782314; and 5P that binds to the + strand from 108764295–108764762. Upon Southern blot confirmation, the PGK-Neo selection cassette was removed from the targeting allele by crossing the wt/PGK-Neo-flox mice with C57BL/6 FLPe deleter mice.

Generation and genotyping of *Maspin* KO mice

The animal protocol was approved by Institutional Animal Care and Use Committee in compliance with the animal welfare guidelines. A female Zp3-Cre transgenic mouse strain C57BL/6-TgN(Zp3-Cre)93Knw was purchased from the Jackson Laboratory (Bar Harbor, ME). To generate homozygous *Maspin* KO (i.e., Δ/Δ) mice, cross-breeding was performed according to two different schemes as illustrated in Fig. 2A. For routine genotyping, genomic DNA was isolated from tails of mice before weaning, using the DirectPCR Lysis Reagent (Viagen Biotec, Los Angeles, CA) and amplified by PCR using the HotStarTaq Master Mix (Qiagen, Valencia, CA). Table S1 lists the genotyping PCR primer sequences and the corresponding expected product sizes. The PCR reaction consisted of 35 cycles of initial heat activation at 95 °C for 15 min → annealing at 57 °C for 60 s → extension at 72 °C for 60 s, followed by a final extension step at 74 °C for 10 min. The PCR products were resolved by electrophoresis on a 2% agarose gel and visualized by ethidium bromide staining.

Detection of mRNA by quantitative real time PCR (qRT-PCR)

Total RNA was extracted from snap frozen mouse tissues and the pair of *Pten*$^{+/+}$ and *Pten*$^{-/-}$ prostate epithelial cell lines (16) using the RNeasy Mini Kit (Qiagen Valencia, CA). One microgram of each RNA sample was reverse-transcribed using the iScript cDNA Synthesis kit (Bio-Rad, Irvine, CA). The qRT-PCR of maspin was performed using a Bio-Rad iQ™5 Multicolor RT-PCR system as previously described (10), using the primers listed in Table S1. The primers for mouse GAPDH and HDAC1 were described previously (10, 30). The amplified maspin PCR products were visualized and semi-quantitatively analyzed by agarose gel electrophoresis and densitometric quantification using ImageJ program, a public domain image processing software developed at the National Institutes of Health (https://imagej.nih.gov). The relative expression of HDAC 1 mRNA was analyzed by the $2^{(-\Delta\Delta\ Ct)}$ method.

Detection of maspin protein by western blotting (WB)

The snap frozen mouse tissues and the prostate epithelial cells from *Pten*$^{+/+}$ and conditional *Pten*$^{-/-}$ mice were homogenized on ice by sonication and lysed with RIPA buffer as previously described (1). Protein concentration was determined by the BCA Protein Assay Kit (Thermo Fisher Scientific, Hudson, NH). A total of 20 μg of tissue protein were subjected to 12% SDS-polyacrylamide gel electrophoresis and WB using specific antibodies against maspin (Abs4A, (1)), α-tubulin (#ab4074, Abcam), GAPDH (#ab8245, Abcam) and β-actin (SC47778, Santa Cruz). Densitometric analysis of the WB protein was performed using the ImageJ software.

cDNA sequence identification

cDNA amplified by PCR was extracted from the agarose electrophoresis gel using QIAquick Gel Extraction Kit (Qiagen, Valencia, CA). The Sanger sequencing was performed by the Applied Genomics Technology Center (AGTC, WSU). Sequence search was performed using the nucleotide BLAST tool publicly available at http://blast.ncbi.nlm.nih.gov/Blast.cgi.

Analysis of Animal Growth

Mice were weighted two times every week for the first 10 weeks. A non-linear three parameter least-squares random effect model was used to compare the growths of different genotypes and different genders. The three parameters were: the upper asymptote (the maximum body weight, MBW), scale (growth rate), and inflection point (time point of ½ MBW). The lower asymptote (response value at negative infinite time) was set to 0. A P value of < 0.001 is considered statistically significant.

Mouse tissue histopathology and immunohistochemistry (IHC)

Tissues were fixed in formaldehyde, paraffin embedded and sectioned as previously described (31). Tissue sections from at least six mice in each genotype group were subjected to both H&E stain, and IHC using maspin-specific Abs4A antibody as previously described (31). All slides were analyzed by our pathologists whose contributions are specified in the Authors' Contribution section.

New animal models/resource sharing

The *Maspin*$^{flox/\Delta}$ and *Maspin*$^{\Delta/\Delta}$ mice will be made available as long as they are being used in the author's laboratory or in collaboration with the authors, and as long as the requesters do not intend to use them for commercial purposes.

Results

Inactivation of *Maspin* gene in the oocyte is embryonically lethal but can be circumvented by an alternative breeding scheme

The *Maspin* gene, located on mouse chromosome 1, is composed of 7 exons (Fig. 1 A & B). Previously, it was shown that targeted deletion of exons 4 or 7 effectively abolished maspin expression. In this study, we chose to target *Maspin* by a custom-designed targeting vector that flanks *Maspin* exon 4 with two loxP sites (Fig. 1C) in a manner similar to that reported by Teoh *et al.* (19). Based on the structural information (32), targeting *Maspin* exon 4 will delete the α-helices E and F, which are essential for stabilizing both the serpin structural frame and the RCL (Fig. 1A and Fig. 1S A & B). In the absence of exon 4, the protein is not expected to fold properly and should therefore be unstable. Southern blot analysis (Fig. 1F) and PCR-based genotyping (Fig. 1G) confirmed germ line transmission of the floxed allele resulting from the removal of the neo cassette by crossing *Maspin*$^{wt/PGK\text{-}Neo\ flox}$ mice with C57BL/6J FLPe deleter mice (Fig. 1D). The resulting flox homozygous mice were fertile. To delete the *Maspin* gene prior to embryogenesis (Fig. 1E), we utilized C57BL/6-Tg(Zp3-Cre)93Knw/J transgenic mouse strain where Cre expression was under the regulation of

oocyte-specific *Zona Pellucida 3* (*Zp3*) promoter. The Zp3 protein is a sperm receptor produced by oocyte during the first meiotic division, to facilitate the sperm binding and the injection of the sperm DNA into the egg. It has been shown that the Zp3-Cre-mediated gene-targeting occurs prior to fertilization and is highly efficient (33).

To ascertain whether the survival of *Maspin* KO reported by Teoh *et al.* (19) results from off-target effects of the genomic insertion of loxP sites, which are shown to not only increase interchromosomal rearrangement but also to alter the epigenetic gene expression profile (34), we designed two breeding schemes for conditional *Maspin* deletion (Fig. 2A). In Scheme 1, to simulate the homologous recombination-based *Maspin* gene deletion in ESC as reported by Gao *et al.* (26), we back-crossed F1 Cre^{+};wt/flox females (donors of wt/Δ oocyte) with wt/wt male mice to generate F2 wt/Δ mice, which were then intercrossed to generate the F3 offspring. In breeding Scheme 2, which was similar to the procedure described by Teoh *et al.* (19), F1 Cre^{+};wt/flox females were backcrossed with flox/flox male mice to generate flox/Δ mice (F2), which were intercrossed to generate F3 offspring. The number of litters, number of pups and gender distributions of the F2 and F3 offspring are summarized in Table S2. Based on PCR genotyping (Fig. 2B & Table 1), the Zp3-Cre-controlled *Maspin* deletion was achieved predominantly prior to fertilization, since among 69 F2 offspring analyzed from both breeding schemes only one Cre^{+};wt/flox/Δ mosaic animal was identified. Based on the complete absence of live births of Δ/Δ mice from breeding Scheme 1, we unequivocally confirmed the embryonic lethality of *Maspin* KO mice. In parallel, the evidence that breeding Scheme 2 produced Δ/Δ F3 mice in Mendelian ratio relative to other flox/flox and flox/Δ genotypes is consistent with the report of Teoh *et al.* (19).

Inactivation of *Maspin* gene abrogates maspin expression

To examine the effects of *Maspin* gene deletion on maspin protein expression, we chose to use tissues from virgin mice to avoid skewing the basis for quantitative comparison, although the detection of maspin may be easier in some tissues, e.g. mammary gland, in pregnant mice (35, 36). Earlier, we showed that maspin is expressed in prostate epithelial cells, $Pten^{+/+}$, but not in $Pten^{-/-}$ (16). As shown in Fig. 3A(a), the maspin band was the only protein detected by WB using the Abs4A antibody in the $Pten^{+/+}$ but not $Pten^{-/-}$ cells. These data demonstrate the specificity of our maspin antibody. In parallel, maspin was detected in the mammary tissues of wt/wt mice, but was significantly decreased and undetectable in the mammary tissues of flox/Δ and Δ/Δ mice, respectively (Fig. 3A(a) & (b)). Similar to the observed tissue-specific expression patterns in human tissues, maspin was not detected in the skeletal muscle tissues across all three genotypes. Consistent with the report of Kouadjo *et al.* (37), housekeeping proteins used in WB as loading controls in human tissue samples seemed to be tissue-specific in mice. GAPDH was abundantly expressed in skeletal muscle, but not in mammary glands. On the other hand, β-actin was expressed in mammary glands, but not in skeletal muscle tissues. The densitometric measurement of maspin confirmed its reduction and loss in flox/Δ and Δ/Δ mice, respectively (Fig. 3A(b)). Interestingly, α-tubulin, another commonly used housekeeping loading control in human cells, was progressively down-regulated in mammary tissues, but not in skeletal muscle tissues, from wt/wt to flox/Δ and to Δ/Δ mice (Fig. 3A(b) & (c)).

As judged by qRT-PCR using the SD-1ac pair of primers (Table S1), maspin mRNA was detectable in the mammary and intestine tissues of wt/wt mice, decreased in flox/Δ mouse tissues and undetectable in Δ/Δ tissues (Fig. 3B(a) & (b)) As shown in Fig. 3B(a), a 180 bp product was the only band detected in *Pten*$^{+/+}$ cells, and was not detected in *Pten*$^{-/-}$ cells, confirming the specificity of the SD-1ac PCR primers for mouse maspin. We also performed qRT-PCR using the primer set PB1687/1688 (Table S1) as described by Teoh *et al.* (19). Although these primers detected maspin in *Pten*$^{+/+}$ cells and mammary tissues of wt/wt mice, they detected a spectrum of nonspecific amplicons in all the samples analyzed (Fig. S2). Interestingly, our SD-1ac primers also specifically amplified another mRNA species of about 550 bp in epithelial tissues of flox/Δ and Δ/Δ mice, but not wt/wt mice. This mRNA species had a higher melting temperature than maspin mRNA for the SD-1ac primers (Fig. S3A) and was sequence-identified as cellular prion protein (PrPC, Fig. S3B) which is known to have pro-survival functions (38). Since in human tumor progression maspin is commonly translocated to the cytosol or down-regulated (12) while HDAC1 is commonly up-regulated (39), we examined whether *Maspin* deletion might lead to increased HDAC1 expression. As shown in Fig 3C, HDAC1 mRNA in the tissues of flox/Δ was variably elevated, and significantly up-regulated ($p<0.01$) in Δ/Δ mouse tissues.

Judging from IHC analysis, wt/wt mammary gland tissues exhibited intense nuclear maspin staining in myoepithelial cells and in the mucinous lumen (Fig 4A(a)), a pattern similar to that observed in human mammary gland epithelium (1). Similarly, maspin was detected as a nuclear protein in the epithelial cells of all three prostate lobes of wt/wt mice (Fig. S4A). The level of maspin was downregulated in mammary gland epithelial cells of female flox/Δ mice. In parallel, the level of maspin was downregulated in the prostate epithelial cells of male flox/Δ mice. Similarly to the IHC negative control with pre-immune IgG (Fig. S4B) and the IHC of maspin in skeletal muscle tissue that did not express maspin (Fig. S4C), IHC detected no maspin protein in Δ/Δ tissues of mammary (Fig. 4A) and prostate (Fig. S4A) tissues.

Maspin KO compromises epithelial differentiation leading to organ specific and cell-type specific atrophy, adenoma, hyperplasia, and carcinoma

Maspin KO globally impacted early growth (in the first 10 weeks), as judged by a three parameter logistic regression model based on the upper asymptote (MBW), the scale (growth rate), and the inflection point (time point at which the estimated weight is half that of the MBW). As compared to wt/wt mice, the Δ/Δ mice were significantly smaller ($P<0.001$) and growth-delayed for 1.1 days (Fig. S5). The flox/Δ mice had even smaller MBW ($P<0.001$) with a longer growth delay (by 3.1 days). Of note, *Maspin* deletion did not alter the gender differences in MBW. Across all three genotypes, male mice were significantly larger compared to female mice ($P<0.001$) and reached MBW 3.7 days sooner ($P<0.001$). Histopathological examination revealed that the testes in male mice and the ovaries in female mice were not altered by *Maspin* deletion (Fig. S6). In addition, non-epithelial tissues such as skeletal muscle tissues had similar histomorphological features across the three genotypes (Fig. S4).

Pathological conditions were noted in the mammary gland, prostate, lung, intestine, and skin of flox/Δ and Δ/Δ mice. As shown in Fig. 4A(a), the mammary glands of all flox/Δ and Δ/Δ females, as early as 6 weeks of age, had stellate configurations with an increased number of myoepithelial cells consistent with hyperplasia. As compared to the mammary tissues of wt/wt female mice, the mammary tissues of both flox/Δ and Δ/Δ females featured a significantly higher number of acini after 20 weeks of age (Fig. 4A(b), $P<0.01$), with the highest number of acini found in the mammary tissues of flox/Δ females ($P<0.01$). Of note, the mammary gland of a 6-week old Δ/Δ female featured a well-circumscribed tumor of 3 mm in maximum dimension (Fig. S7). The cell clusters and sheets contained many groups exhibiting cytoplasm with a micro-vesicular pattern, reminiscent of sebaceous differentiation. Judging from the low nuclear grade, lack of nuclear pleomorphism, mitosis and necrosis, the histology is consistent with sebaceous adenoma.

As early as 6-weeks of age each of the three prostate lobes of flox/Δ and Δ/Δ mice identified based on the anatomical and histological features of wt/wt prostate (Fig S8), displayed extensive and cell type specific alteration of epithelial differentiation. As shown in Fig. 4B, each Δ/Δ dorsolateral (DLP) lobe examined uniformly exhibited features of hyperplasia, which includes budding intraluminal projection with centrally located and enlarged nuclei, a lack of epithelial aligning at the basolateral side, and fibromuscular stroma. The hyperplastic lesions detected in flox/Δ DLP were less pronounced as compared to that in Δ/Δ DLP. As compared to the papillary or cribriform patterns of wt/wt anterior lobe prostate (AP), the Δ/Δ AP displayed hyperplasia, mild cytological atypia and anastomosis with dilated epithelia and increased papillary projections. Interestingly, the AP lumen of flox/Δ mice was significantly enlarged and filled with immature and sloughing cells. The flox/Δ ventral prostate (VP) appeared to be similar to the wt/wt VP. However, the VP of Δ/Δ mice were significantly enlarged and dilated with flattened atrophic cells with small cell body and small nuclei.

Maspin deletion did not affect early lung development (Fig 5A). At one-year of age, all 9 wt/wt mice examined showed no histopathological findings. However, 2 out of 9 KO mice (22.2%) spontaneously developed peripheral nodules, measuring 0.35 and 1.2 mm in the greatest dimension, respectively. These nodules showed greatly enlarged pneumocytes growing along intact alveoli, and were indistinguishable from lesions which in humans would be classified as adenocarcinoma with an exclusively lepidic growth pattern (40). In addition, they perfectly matched neoplastic proliferations occurring in *in vivo* models of adenocarcinoma (41, 42), particularly fitting into grades 2 and 3 (the smaller and the larger tumor, respectively), of a proposed 5 tier histological model of adenocarcinoma progression (43) (Fig. 5B(a), (b) & (c)).

We also examined the impact of *Maspin* deletion on small intestine (SI) and skin. As compared to SI of wt/wt mice, the SI of Δ/Δ and flox/Δ mice exhibited a distorted ratio between glandular *versus* fibromuscular tissues and dilated submucosa with increased presence of inflammatory cells (Fig. S9). While the skin of wt/wt mice consisted of dermis with dense connective tissue with small blood vessels, the skin of Δ/Δ 10-weeks old mice was characterized by focal thinning of the epidermis (1–2 layers of cells), loss of epidermal stratification (specifically stratum spinosum), decreased presence of sebaceous glands and hair follicles, and loosened connective tissue in dermis (Fig. 6A). These histomorphological

changes were associated with the development of Alopecia aerate in both male and female Δ/Δ mice (Fig. 6B).

Discussion

The employment of floxed founder mice in two complementary breeding schemes in this study was critical to resolve the controversy regarding the role of maspin in embryogenesis and tumor development. Results from our cross-breeding Scheme 1 and the results of Gao *et al.* (26) consistently show that embryonic lethality occurs with 100% penetrance when the first heterozygous *Maspin* deletion is introduced in the presence of a wild type sister allele in either ESC or during oogenesis. These data indicate that no redundant proteins or mechanisms can compensate for the unique biological functions of maspin in embryogenesis.

Earlier, we have shown that maspin inhibits HDAC1 (3, 7), which is also essential for embryogenesis (44). The biological activities of HDAC1 in embryogenesis appear to be distinct among HDAC isoforms and may differ from the HDAC1 functions in somatic cells of various differentiation lineages (45). Future studies are warranted to address whether the lack of maspin-mediated control of HDAC1 activity underlies the embryonic lethality of *Maspin* KO mice, and whether the cell type-specific expression of maspin and its inhibitory interaction with HDAC1 in embryogenesis are distinct from those in somatic tissues. More importantly, considering the evidence that *Maspin* deletion led to spontaneous epithelial abnormalities ranging from hyperplasia to carcinoma, reminiscent to the continuum of human tumor progression, our finding that *Maspin* deletion also led to increased HDAC1 expression is not only consistent with the clinical evidence, but also supports an intriguing possibility that maspin differential expression may be a driver of the HDAC-mediated epigenetic changes in tumor cells.

Our genotyping confirmed the intended targeted maspin deletion in flox/Δ and Δ/Δ mice (Fig. 2). Maspin is generally expressed in an epithelial-specific manner and is not an imprinted gene (46). Thus, the circumvention of *Maspin* KO embryonic lethality in cross-breeding Scheme 2 or in the study of Teoh *et al*. (19) was not likely due to parent-of-origin. While the full impact of loxP site insertion remains to be systematically interrogated, the flox/flox mice expressed maspin at a level similar to that of wt/wt (data not shown), indicating that loxP site insertion by itself did not alter the Cre-mediated targeted *Maspin* deletion or maspin expression. Further, maspin expression showed dose-dependent decrease from wt/wt to flox/Δ mice and was undetectable in Δ/Δ mice, indicating that the loxP site in flox/Δ mice did not lead to overcompensation for the loss of *Maspin per se*. However, our data do not exclude the possibility that a floxed *Maspin* allele may have changed the genomic or epigenetic context of *Maspin* deletion in the sister allele, thus subsequently allowing for the Δ/Δ offspring to survive. Indeed, a recent study showed that loxP site insertion into chromosome altered gene transcription, possibly through changes of chromosomal conformation (34). Further, consistent with this notion was our incidental finding that PrPC was absent in wt/wt mice but was more upregulated in flox/Δ mice than in Δ/Δ mice. The expression of PrPC is known to be responsive to chromatin structural instability and act to protect cell viability (38).

Our flox/Δ and Δ/Δ mice exhibited widespread and significant pathological conditions (Fig. 4–6 & Fig. S4–S9). The differences between our data and the results of Teoh *et al.* may be due, at least in part, to differences in experimental quality control. First, Teoh *et al.* used chimeric mice to cross with CMV-Cre-deleter mice without first confirming the germline transmission of the floxed allele (19), which is likely to increase the degree of mosaicism in the resulting "*Maspin* KO mice". To this end, the PCR primers used by Teoh *et al.* proved to lack specificity for maspin cDNA (Fig. S3), whereas, as acknowledged by the authors, their maspin antibody cross-reacted with multiple non-specific proteins (19). Taken together, these technical issues raise concerns about the purity of the genotype and the certainty of the phenotype of the *Maspin* KO mice in the study of Teoh *et al*. In our study, we confirmed the germline transmission of the floxed allele and removed the PGK-Neo selection cassette before backcrossing F1 Cre^{+};wt/flox females with flox/flox male mice to generate F2 flox/Δ mice (Fig. 2A). Our genotyping (Fig. 2B), maspin mRNA detection by qRT-PCR with highly specific probes, and WB and IHC detection of maspin protein with a highly specific maspin antibody (Fig. 3 & 4), consistently demonstrated the purity of the flox/Δ and Δ/Δ genotypes. Secondly, our phenotypic analysis was significantly expanded from that reported by Teoh *et al*., which was limited to the skin tissues of 8-weeks old wt/wt and Δ/Δ mice (19). Our study covered multiple time points in the first year of mouse lives, 7 different organs, three genotypes (wt/wt and flox/Δ and Δ/Δ) and both genders.

The phenotypic changes observed in somatic tissues of our flox/Δ and Δ/Δ mice demonstrate that the mechanism underlying the survival of *Maspin* KO mice in Scheme 2 cannot fully compensate the unique functional loss of maspin in epithelial development and pathogenesis. Based on the evidence derived from maspin haploinsufficiency in the prostate (hyperplasia), intestine (distorted ratio of glandular epithelium versus fibromuscular stoma) and mammary gland (hyperplasia), and *Maspin* deletion in mammary gland (adenoma and hyperplasia), lungs (adenocarcinoma), prostate (lobe specific hyperplasia or atrophy) and skin (atrophy and Alopecia aerate), it is clear that *Maspin* deletion is causatively involved in the corresponding pathobiological processes. Interestingly, the flox/Δ AP lobes showed more severe histopathology when compared to the age-matched Δ/Δ tissues (Fig. 4B). In addition, the flox/Δ mammary gland featured more severe myoepithelial hyperplasia and a higher number of mammary gland acini compared to Δ/Δ mice (Fig. 4A). In these cases, it is conceivable that the compensatory response to *Maspin* haploinsufficiency may involve a factor (yet to be identified) that is both partially redundant with and partially competitive against maspin, leading to more dramatic changes than those observed in KO tissues where such antagonism is absent due to the homozygous loss of maspin.

The generation of live flox/Δ and Δ/Δ mice using Scheme 2 allowed us not only to demonstrate the potential of maspin to suppress the development of cancer where differential expression of maspin has been linked to disease progression, but also to dissect the temporal impacts of organ- and cell-type specific functions of maspin. The most aggressive type of tumor developed in KO mice was lung adenocarcinoma despite the fact that C57BL mouse genetic background rarely supports lung tumor development (47). The lung adenocarcinoma in KO mice was similar to the adenocarcinoma in other well-established genetic models of lung cancer (41, 42) and, more importantly, were indistinguishable from lesions which in humans would be classified as adenocarcinoma with

an exclusively lepidic growth pattern (40). To determine whether these tumors have the *bona fide* traits of cancer tissues, future experiments need to include the characterization of the transplants of these tumors in syngeneic mouse hosts.

Starting at puberty, all the flox/Δ and Δ/Δ mice examined exhibited significant pathologic features in the mammary gland or prostate in cell-type specific manner or lobe-specific manner (Fig. 4) In the prostate, *Maspin* deletion resulted in luminal-cell hyperplasia in the AP lobe and luminal-cell atrophy of the VP lobe. Importantly, both flox/Δ and Δ/Δ mice developed hyperplastic lesions in DLP that closely resemble PIN lesions in the peripheral zone of the human prostate (48). This result is similar to that reported by Shao *et al.* with $Maspin^{wt/\Delta}$ mice (27), and independently validates the specificity of the maspin effects. In normal human breast tissues, maspin is highly expressed in myoepithelial cells which have been shown to act as a natural defense against breast cancer (49). It is not surprising that *Maspin* deletion resulted in increased proliferation and dedifferentiation of myoepithelial cells. The concomitant down-regulation of α-tubulin and the myoepithelial hyperplasia in flox/Δ and Δ/Δ mice (Fig. 3B) is consistent with the notion that mammary gland cancer stem-like cells for aggressive basal cell type or $ER^{-}/PR^{-}/Her\text{-}2^{-}$, also known as triple negative mammary gland cancer, may reside in the myoepithelial layer and may be marked by the down regulation of α-tubulin (50–53).

As our results clearly demonstrate a role of epithelial-specific maspin as a tumor suppressor, it is important to note that in human tumor progression maspin down-regulation is usually preceded by maspin translocation from the nucleus to the cytoplasm (11, 36, 54). Future investigations need to recapitulate maspin temporal and spatial regulation in clinically relevant biological sequence. On the other hand, our data linked maspin differential expression in epithelial cells to host immune response and support our earlier notion that maspin re-expression in prostate tumor cells augmented innate and humoral antitumor immunity to increase tumor elimination *in vivo* (31). Further, the skin pathology and Alopecia aerate incidents in KO mice are in line with the evidence that maspin acts as an autoantigen in HLA-Cw6-associated T-cell-mediated psoriasis, a persistent autoimmune disease of the skin (55).

Our *Maspin* KO model will be a valuable tool to recapitulate clinically relevant human pathologies. As the only endogenous HDAC1 inhibitor identified thus far, the value of our *Maspin* KO model in studying the role of maspin in epithelial differentiation or tumor development will be far reaching. The *Maspin* KO mice will be particularly useful to fill a gap of knowledge about how dysregulation of HDAC1 and its associated transcriptome landscape may drive tumor progression. We noted that the spontaneous tumor formation in *Maspin* KO mice occurs at a relatively low rate. However, it is likely that the loss of control by maspin of HDAC1-mediated epigenetic programs may be pleiotropic to exacerbate tumor development and progression initiated by other oncogenic mechanisms. The identification of organs and cell types where maspin loss spontaneously induces epithelial abnormalities and tumor development will undoubtedly provide a clear road map for how the mechanistic interplay between maspin and HDAC1 should be further investigated in a controlled fashion (e.g. ectopic viral infection) in specific organ sites, such as lung, prostate, mammary gland or intestine. In summary, this study clearly resolved the controversy raised by two previous

studies regarding the role of maspin in embryogenesis and tumorigenesis. Importantly, our new results demonstrate that maspin is a powerful context-dependent tumor suppressor and support the development of maspin-based therapeutics for cancer treatment.

Supplementary Material

Refer to Web version on PubMed Central for supplementary material.

Acknowledgments

We acknowledge Ms. Maria Matta for her critical proofreading of this manuscript.

Financial support: This work was supported by NIH grants (CA127735 and CA084176 to Sheng, S.), Fund for Cancer Research (to Sheng, S. and Heath, E.), and the Ruth Sager Memorial Fund (to Sheng, S.), the Wayne State University Vice President Office for Research (to Sheng, S.), and NIH grant P30 CA022453 (to Karmanos Cancer Institute with Sheng, S. as a program leader). The NIH grant P30 CA022453 also supports the Wayne State University and Karmanos Cancer Institute Applied Genomics Technology Center.

References

1. Zou ZQ, Anisowicz A, Hendrix MJC, Thor A, Neveu M, Sheng SJ, et al. Maspin, a Serpin with Tumor-Suppressing Activity in Human Mammary Epithelial-Cells. Science. 1994; 263:526–529. [PubMed: 8290962]
2. Futscher BW, Oshiro MM, Wozniak RJ, Holtan N, Hanigan CL, Duan H, et al. Role for DNA methylation in the control of cell type specific maspin expression. Nat Genet. 2002; 31:175–179. [PubMed: 12021783]
3. Dzinic SH, Kaplun A, Li XH, Bernardo M, Meng YH, Dean I, et al. Identification of an Intrinsic Determinant Critical for Maspin Subcellular Localization and Function. PLoS One. 2013; 8
4. Al-Ayyoubi M, Gettins PGW, Volz K. Crystal structure of human maspin, a serpin with antitumor properties - Reactive center loop of maspin is exposed but constrained. The Journal of Biological Chemistry. 2004; 279:55540–55544. [PubMed: 15501821]
5. Law RH, Irving JA, Buckle AM, Ruzyla K, Buzza M, Bashtannyk-Puhalovich TA, et al. The high resolution crystal structure of the human tumor suppressor maspin reveals a novel conformational switch in the G-helix. The Journal of Biological Chemistry. 2005; 280:22356–22364. [PubMed: 15760906]
6. Benarafa C, Remold-O'Donnell E. The ovalbumin serpins revisited: perspective from the chicken genome of clade B serpin evolution in vertebrates. Proceedings of the National Academy of Sciences of the United States of America. 2005; 102:11367–11372. [PubMed: 16055559]
7. Li X, Yin S, Meng Y, Sakr W, Sheng S. Endogenous inhibition of histone deacetylase 1 by tumor-suppressive maspin. Cancer Research. 2006; 66:9323–9329. [PubMed: 16982778]
8. Laugesen A, Helin K. Chromatin repressive complexes in stem cells, development, and cancer. Cell Stem Cell. 2014; 14:735–751. [PubMed: 24905164]
9. Kidder BL, Palmer S. HDAC1 regulates pluripotency and lineage specific transcriptional networks in embryonic and trophoblast stem cells. Nucleic Acids Research. 2012; 40:2925–2939. [PubMed: 22156375]
10. Bernardo MM, Meng Y, Lockett J, Dyson G, Dombkowski A, Kaplun A, et al. Maspin reprograms the gene expression profile of prostate carcinoma cells for differentiation. Genes and Cancer. 2011; 2:1009–1022. [PubMed: 22737267]
11. Pierson CR, McGowen R, Grignon D, Sakr W, Dey J, Sheng SJ. Maspin is up-regulated in premalignant prostate epithelia. Prostate. 2002; 53:255–262. [PubMed: 12430137]
12. Lonardo F, Guan H, Dzinic S, Sheng S. Maspin expression patterns differ in the invasive versus lepidic growth pattern of pulmonary adenocarcinoma. Histopathology. 2014; 65:757–763. [PubMed: 25040445]

13. Lonardo F, Li XH, Siddiq F, Singh R, At-Abbadi M, Pass HI, et al. Maspin nuclear localization is linked to favorable morphological features in pulmonary adenocarcinoma. Lung Cancer. 2006; 51:31–39. [PubMed: 16159682]
14. Wang Y, Sheng SJ, Zhang JZ, Dzinic S, Li SL, Fang F, et al. Elevated Maspin Expression Is Associated with Better Overall Survival in Esophageal Squamous Cell Carcinoma (ESCC). PLoS One. 2013; 8
15. Xia WY, Lau YK, Hu MCT, Li L, Johnston DA, Sheng SJ, et al. High tumoral maspin expression is associated with improved survival of patients with oral squamous cell carcinoma. Oncogene. 2000; 19:2398–2403. [PubMed: 10828881]
16. Bernardo MM, Kaplun A, Dzinic SH, Li XH, Irish J, Mujagic A, et al. Maspin Expression in Prostate Tumor Cells Averts Stemness and Stratifies Drug Sensitivity. Cancer Research. 2015; 75:3970–3979. [PubMed: 26208903]
17. Cher ML, Biliran HR, Bhagat S, Meng YH, Che MX, Lockett J, et al. Maspin expression inhibits osteolysis, tumor growth, and angiogenesis in a model of prostate cancer bone metastasis. Proceedings of the National Academy of Sciences of the United States of America. 2003; 100:7847–7852. [PubMed: 12788977]
18. Sheng SJ, Pemberton PA, Sager R. Production, Purification, and Characterization of Recombinant Maspin Proteins. The Journal of Biological Chemistry. 1994; 269:30988–30993. [PubMed: 7983035]
19. Teoh SSY, Vieusseux J, Prakash M, Berkowicz S, Luu J, Bird CH, et al. Maspin is not required for embryonic development or tumour suppression. Nature Communications. 2014; 5
20. Zhang H, Xie Y, Li W, Chibbar R, Xiong S, Xiang J. CD4(+) T cell-released exosomes inhibit CD8(+) cytotoxic T-lymphocyte responses and antitumor immunity. Cellular and Molecular Immunology. 2011; 8:23–30. [PubMed: 21200381]
21. Zhang M, Sheng SJ, Maass N, Sager R. mMaspin: The mouse homolog of a human tumor suppressor gene inhibits mammary tumor invasion and motility. Molecular Medicine. 1997; 3:49–59. [PubMed: 9132279]
22. Zhang M, Shi Y, Magit D, Furth PA, Sager R. Reduced mammary tumor progression in WAP-TAg/WAP-maspin bitransgenic mice. Oncogene. 2000; 19:6053–6058. [PubMed: 11146557]
23. Luo JL, Tan W, Ricono JM, Korchynskyi O, Zhang M, Gonias SL, et al. Nuclear cytokine-activated IKKalpha controls prostate cancer metastasis by repressing Maspin. Nature. 2007; 446:690–694. [PubMed: 17377533]
24. Shi HY, Liang R, Templeton NS, Zhang M. Inhibition of breast tumor progression by systemic delivery of the maspin gene in a syngeneic tumor model. Molecular Therapy. 2002; 5:755–761. [PubMed: 12027560]
25. Abraham S, Zhang WG, Greenberg N, Zhang M. Maspin functions as a tumor suppressor by increasing cell adhesion to extracellular matrix in prostate tumor cells. J Urology. 2003; 169:1157–1161.
26. Gao F, Shi HY, Daughty C, Cella N, Zhang M. Maspin plays an essential role in early embryonic development. Development. 2004; 131:1479–1489. [PubMed: 14985257]
27. Shao LJ, Shi HY, Ayala G, Rowley D, Zhang M. Haploinsufficiency of the maspin tumor suppressor gene leads to hyperplastic lesions in prostate. Cancer Research. 2008; 68:5143–5151. [PubMed: 18593913]
28. Kontgen F, Suss G, Stewart C, Steinmetz M, Bluethmann H. Targeted disruption of the MHC class II Aa gene in C57BL/6 mice. International Immunology. 1993; 5:957–964. [PubMed: 8398989]
29. Banati RB, Middleton RJ, Chan R, Hatty CR, Kam WW, Quin C, et al. Positron emission tomography and functional characterization of a complete PBR/TSPO knockout. Nature Communications. 2014; 5:5452.
30. Huang Y, Cai LW, Yang R. Expression of maspin in the early pregnant mouse endometrium and its role during embryonic implantation. Comperative Medicine. 2012; 62:179–184.
31. Dzinic SH, Chen K, Thakur A, Kaplun A, Bonfil RD, Li X, et al. Maspin expression in prostate tumor elicits host anti-tumor immunity. Oncotarget. 2014; 5:11225–11236. [PubMed: 25373490]
32. Gettins PG. The F-helix of serpins plays an essential, active role in the proteinase inhibition mechanism. FEBS Lett. 2002; 523:2–6. [PubMed: 12123794]

33. Lewandoski M, Wassarman KM, Martin GR. Zp3-cre, a transgenic mouse line for the activation or inactivation of loxP-flanked target genes specifically in the female germ line. Current Biology. 1997; 7:148–151. [PubMed: 9016703]
34. Meier ID, Bernreuther C, Tilling T, Neidhardt J, Wong YW, Schulze C, et al. Short DNA sequences inserted for gene targeting can accidentally interfere with off-target gene expression. Faseb Journal. 2010; 24:1714–1724. [PubMed: 20110269]
35. Bailey CM, Margaryan NV, Abbott DE, Schutte BC, Yang B, Khalkhali-Ellis Z, et al. Temporal and spatial expression patterns for the tumor suppressor Maspin and its binding partner interferon regulatory factor 6 during breast development. Development, Growth & Differentiation. 2009; 51:473–481.
36. Zhang M, Magit D, Botteri F, Shi HY, He K, Li M, et al. Maspin plays an important role in mammary gland development. Developmental Biology. 1999; 215:278–287. [PubMed: 10545237]
37. Kouadjo KE, Nishida Y, Cadrin-Girard JF, Yoshioka M, St-Amand J. Housekeeping and tissue-specific genes in mouse tissues. BMC Genomics. 2007; 8:127. [PubMed: 17519037]
38. Westergard L, Christensen HM, Harris DA. The cellular prion protein (PrPC): Its physiological function and role in disease. Biochimica Et Biophysica Acta-Molecular Basis of Disease. 2007; 1772:629–644.
39. Muller BM, Jana L, Kasajima A, Lehmann A, Prinzler J, Budczies J, et al. Differential expression of histone deacetylases HDAC1, 2 and 3 in human breast cancer - overexpression of HDAC2 and HDAC3 is associated with clinicopathological indicators of disease progression. Bmc Cancer. 2013; 13
40. Travis WD, Brambilla E, Nicholson AG, Yatabe Y, Austin JH, Beasley MB, et al. The 2015 World Health Organization Classification of Lung Tumors: Impact of Genetic, Clinical and Radiologic Advances Since the 2004 Classification. J Thorac Oncol. 2015; 10:1243–1260. [PubMed: 26291008]
41. Wang Y, Zhang Z, Lubet RA, You M. A mouse model for tumor progression of lung cancer in ras and p53 transgenic mice. Oncogene. 2006; 25:1277–1280. [PubMed: 16247444]
42. Jackson EL, Willis N, Mercer K, Bronson RT, Crowley D, Montoya R, et al. Analysis of lung tumor initiation and progression using conditional expression of oncogenic K-ras. Genes & Development. 2001; 15:3243–3248. [PubMed: 11751630]
43. Jackson EL, Olive KP, Tuveson DA, Bronson R, Crowley D, Brown M, et al. The differential effects of mutant p53 alleles on advanced murine lung cancer. Cancer Res. 2005; 65:10280–10288. [PubMed: 16288016]
44. Dovey OM, Foster CT, Cowley SM. Histone deacetylase 1 (HDAC1), but not HDAC2, controls embryonic stem cell differentiation. Proceedings of the National Academy of Sciences of the United States of America. 2010; 107:8242–8247. [PubMed: 20404188]
45. Ma P, Schultz RM. HDAC1 and HDAC2 in mouse oocytes and preimplantation embryos: Specificity versus compensation. Cell Death Differ. 2016; 23:1119–1127. [PubMed: 27082454]
46. Morison IM, Reeve AE. A catalogue of imprinted genes and parent-of-origin effects in humans and animals. Hum Mol Genet. 1998; 7:1599–1609. [PubMed: 9735381]
47. Malkinson AM, Nesbitt MN, Skamene E. Susceptibility to urethan-induced pulmonary adenomas between A/J and C57BL/6J mice: use of AXB and BXA recombinant inbred lines indicating a three-locus genetic model. J Natl Cancer Inst. 1985; 75:971–974. [PubMed: 3863994]
48. Berquin IM, Min Y, Wu R, Wu H, Chen YQ. Expression signature of the mouse prostate. The Journal of Biological Chemistry. 2005; 280:36442–36451. [PubMed: 16055444]
49. Sternlicht MD, Kedeshian P, Shao ZM, Safarians S, Barsky SH. The human myoepithelial cell is a natural tumor suppressor. Clinical Cancer Research. 1997; 3:1949–1958. [PubMed: 9815584]
50. Sun BC, Zhang SW, Zhang DF, Li Y, Zhao XL, Luo Y, et al. Identification of Metastasis-Related Proteins and Their Clinical Relevance to Triple-Negative Human Breast Cancer. Clinical Cancer Research. 2008; 14:7050–7059. [PubMed: 18981002]
51. Chao SK, Wang YH, Verdier-Pinard P, Yang CPH, Liu LL, Rodriguez-Gabin A, et al. Characterization of a human beta V-tubulin antibody and expression of this isotype in normal and malignant human tissue. Cytoskeleton. 2012; 69:566–576. [PubMed: 22903939]

52. Orr GA, Verdier-Pinard P, McDaid H, Horwitz SB. Mechanisms of Taxol resistance related to microtubules. Oncogene. 2003; 22:7280–7295. [PubMed: 14576838]

53. Arai K, Nakano H, Shibutani M, Naoi M, Matsuda H. Expression of class II beta-tubulin by proliferative myoepithelial cells in canine mammary mixed tumors. Veterinary Pathology. 2003; 40:670–676. [PubMed: 14608020]

54. Lonardo F, Li X, Kaplun A, Soubani A, Sethi S, Gadgeel S, et al. The natural tumor suppressor protein maspin and potential application in non small cell lung cancer. Current Pharmaceutical Design. 2010; 16:1877–1881. [PubMed: 20337574]

55. Besgen P, Trommler P, Vollmer S, Prinz JC. Ezrin, maspin, peroxiredoxin 2, and heat shock protein 27: potential targets of a streptococcal-induced autoimmune response in psoriasis. Journal of Immunology. 2010; 184:5392–5402.

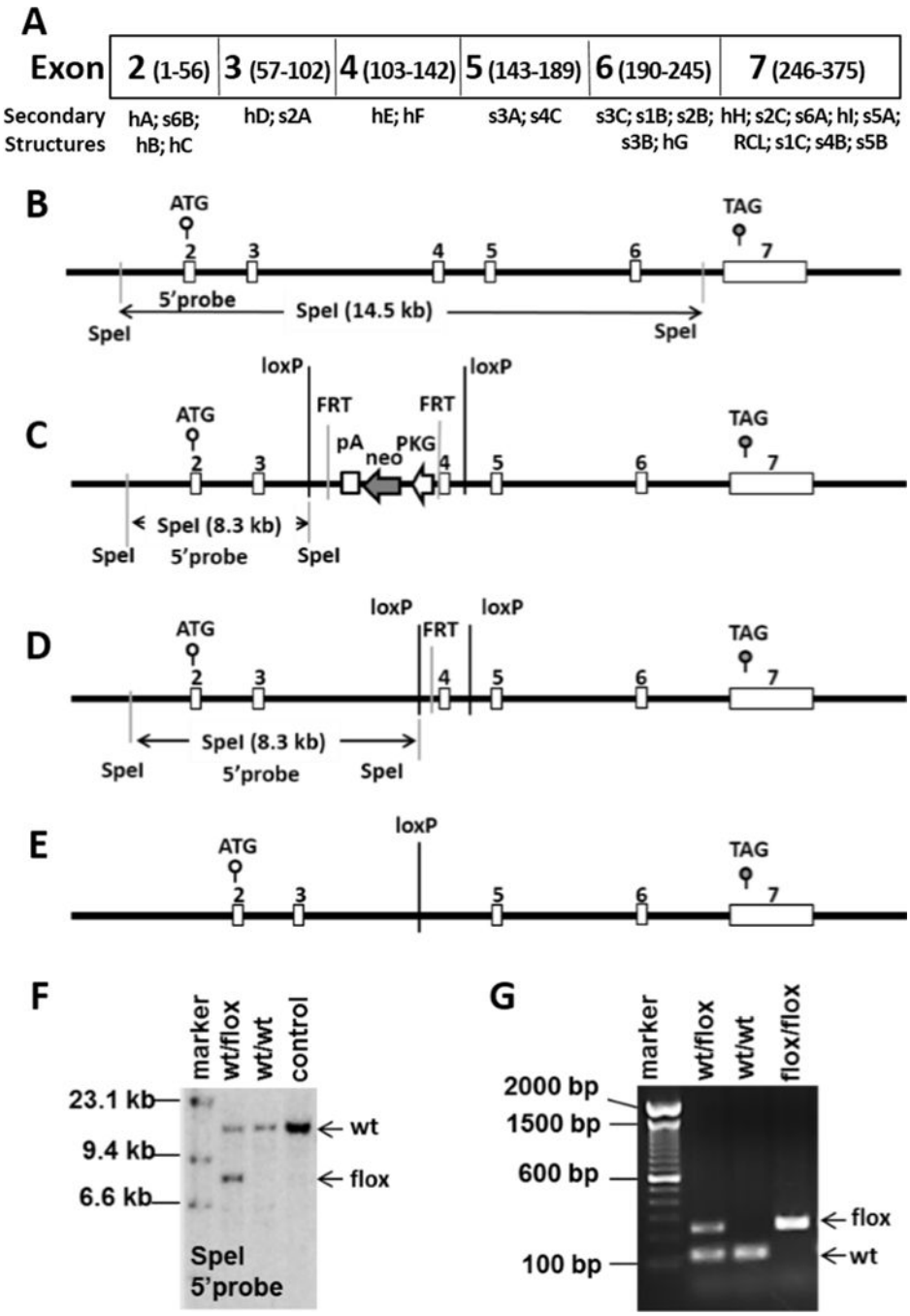

Figure 1. Construction and validation of *Maspin* conditional allele

A, a schematic representation of the mouse maspin coding exons (with the amino acid numbers in parentheses) and the corresponding secondary structural elements. B, a schematic diagram of wt *Maspin* allele. C, diagram of the floxed *Maspin* allele with site-specific insertion of a neomycin cassette (wt/PGK-Neo-flox). D, diagram of the floxed *Maspin* allele after the neomycin cassette is removed. E, diagram of *Maspin* KO allele. F and G are results of Southern blotting or PCR-based genotyping to validate the wt/flox *Maspin* allele, respectively.

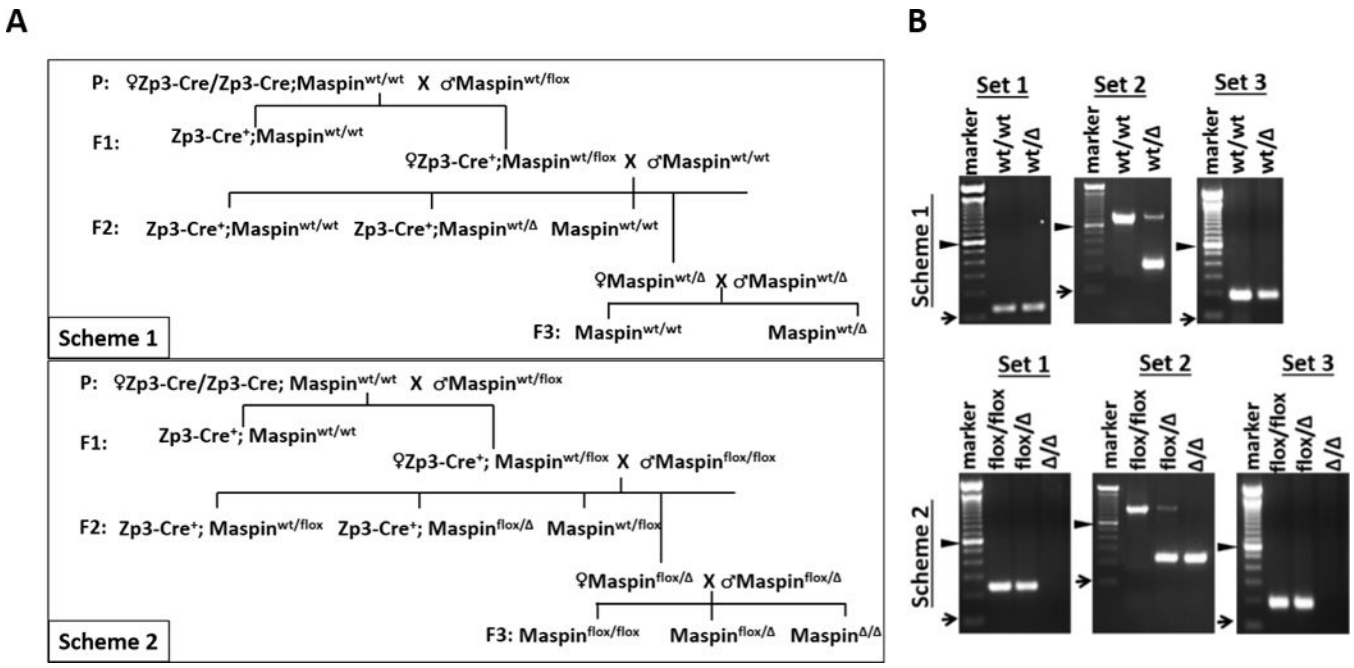

Figure 2. Breeding schemes and genotyping for KO mice

A, two breeding schemes to generate KO mice by mating Cre^{+};wt/flox females with either wt/wt (**Scheme 1**) or flox/flox (**Scheme 2**) males. B, representative results of routine PCR-based genotyping of F3 offspring resulting from **Schemes 1** and **2**. "►" represents 600 bp mark; "➞" represents 100 bp mark. Set 1, Set 2 and Set 3 are PCR primers listed in Table S1.

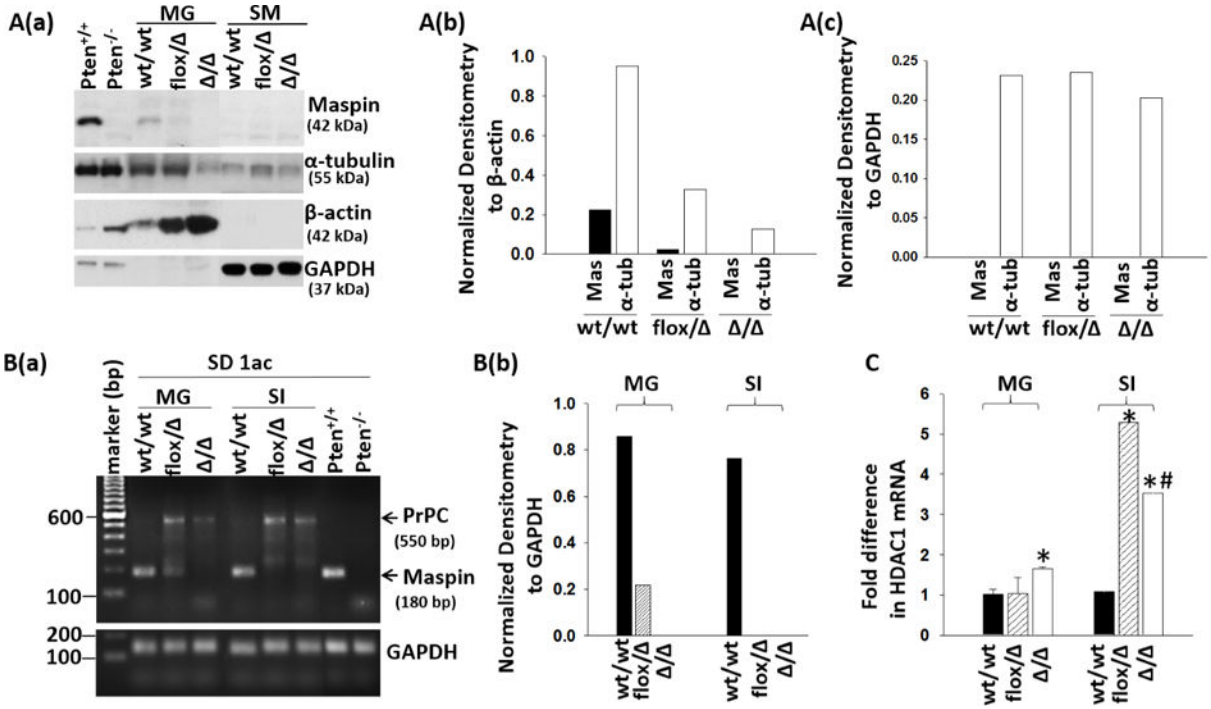

Figure 3. Inactivation of *Maspin* gene abrogates maspin expression

A(a), representative WB of maspin, α-tubulin, β-actin and GAPDH in tissue extracts from mammary gland (MG) and skeletal muscle (SM). (b), densitometric analysis of maspin (mas) and α-tubulin (α-tub) in MG relative to β-actin. (c), densitometric analysis of mas and α-tub in SM relative to GAPDH. (b) and (c) are based on the image of A(a). B(a), detection of maspin, PcPC and GAPDH mRNA by qRT-PCR in mouse tissues. PCR amplicons were resolved by gel electrophoresis. (b), densitometric analysis of maspin mRNA relative to GAPDH. C, detection of HDAC1 mRNA by qRT-PCR. The fold differences in mRNA were calculated by the $2^{(-\Delta\Delta Ct)}$ method using the GAPDH as an internal control. Data represent the average of three repeats and the bars represent the standard errors. "*" and "#" represent statistical significance relative to wt/wt and flox/Δ, respectively ($P < 0.01$).

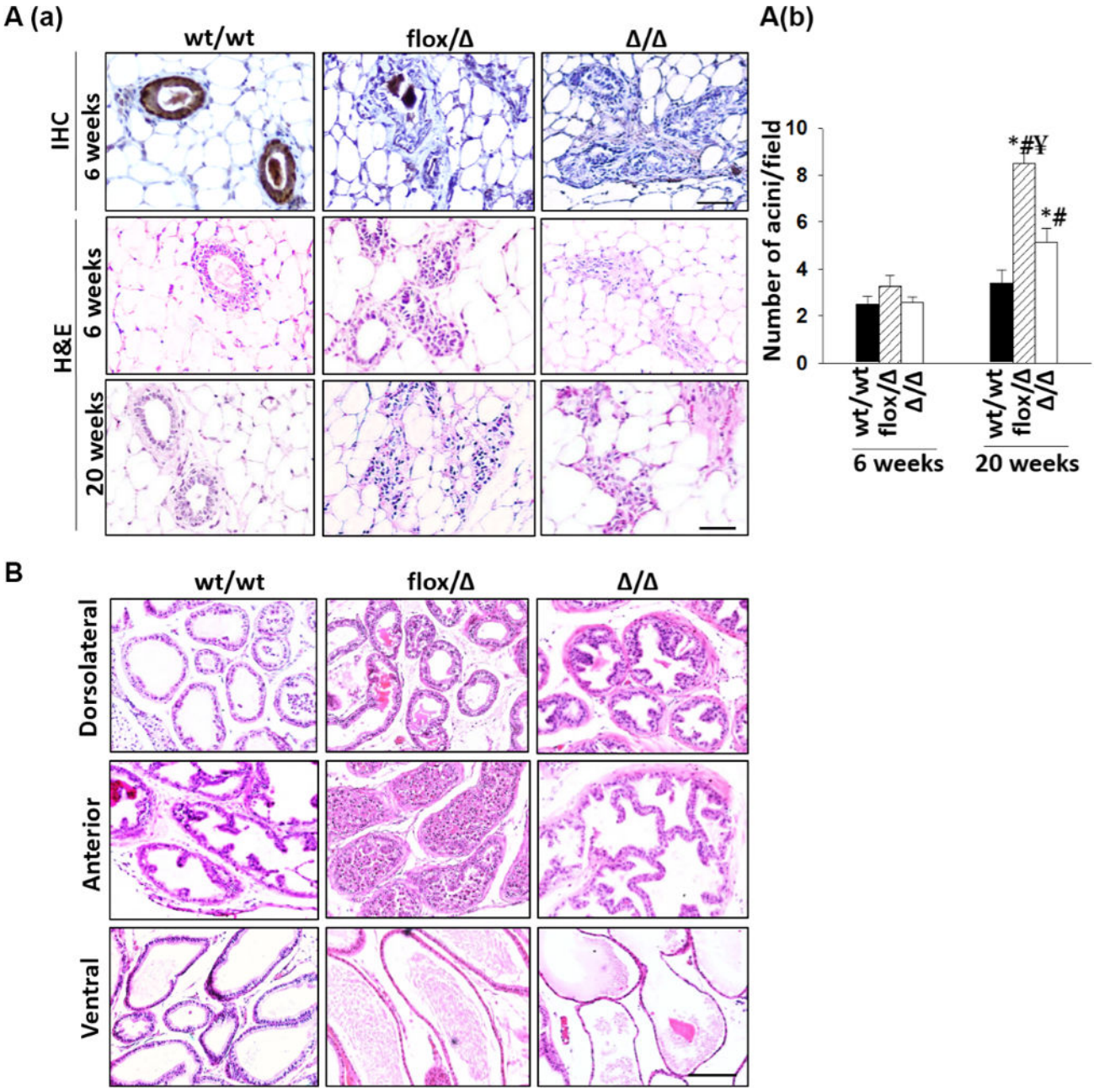

Figure 4. Immunohistopathological analysis of mouse mammary and prostate tissues

A(a), representative H&E and IHC images of mammary tissues of three genotypes. Maspin protein detected by IHC is brown, whereas cell nuclei are counterstained blue. (b), enumeration of mammary gland acini. A minimum of 10 different fields for each mouse and a minimum of 5 mice per genotype were examined by two people and the bars represent the standard errors. Statistical significance based a P value of less than 0.01 was marked by "*" (relative to wt/wt), "#" (relative to the same group from 6-week time point) and "¥" (relative to Δ/Δ). C, representative H&E images of individual prostate lobes of three genotypes. A minimum of 6 mice in each genotype group were examined. (Bar=100 μm).

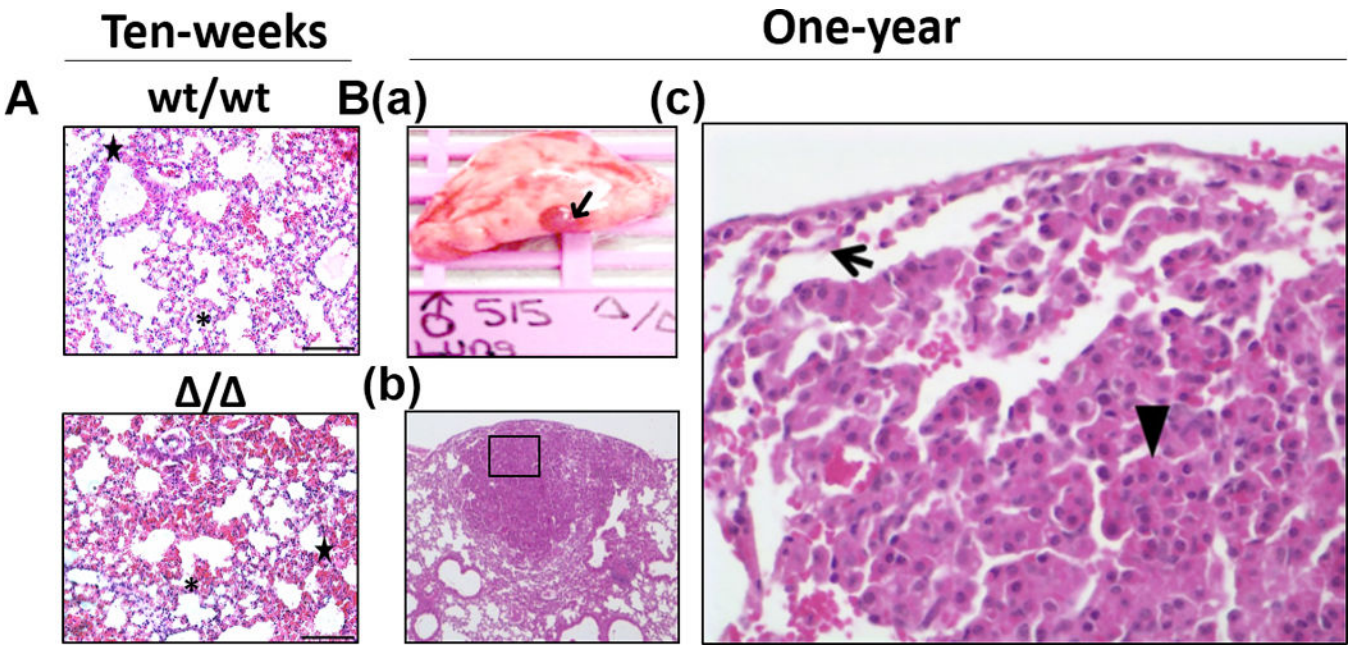

Figure 5. Histopathological analysis of mouse lung tissues

A, Representative low magnification images of H&E stained lung sections from 10-weeks old wt/wt mice and *Maspin* KO mice, respectively, showing no histopathological findings. "*" represents alveoli; "★" represents bronchi. B(a), Gross image of the larger tumor occurring in one-year old KO mouse, visible as a subpleural nodule, (indicated by"➞"). (b) Low magnification of the H&E stained section of the lesion shown in (a). (c) High magnification of the area in the inset of (b). In contrast to the inconspicuous, flat pneumocytes lining normal, patent, subpleural alveoli (marked by "➞"), the pneumocytes of lesional tissue are markedly enlarged and protrude and focally fill alveolar lumens ("►") demonstrating histological features diagnostic of a neoplastic process. (Bar=100 μm).

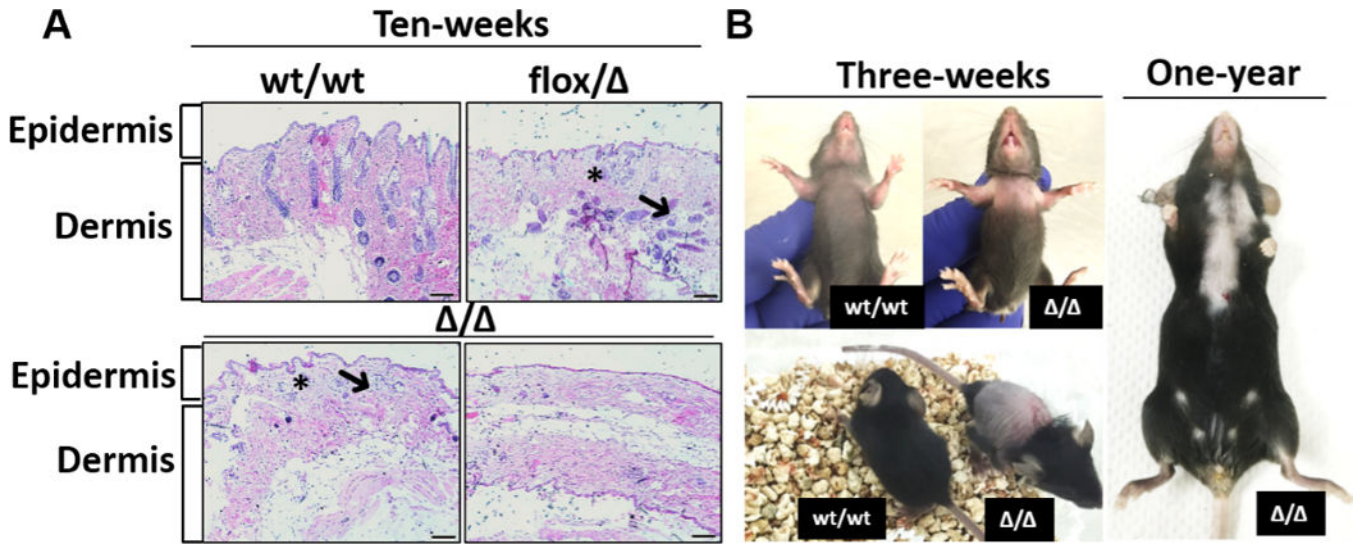

Figure 6. Histopathological analysis of mouse skin tissues

A, representative H&E images of skin tissues from 10-week old mice of three different genotypes. "*" represents sebaceous glands and "➞" represents hair follicles. B, the anterior (left top) and posterior (left bottom) of a 3-week old *Maspin* KO mouse, with age-matched wt/wt as a reference, and a 1-year old *Mapin* KO mouse (right) with Alopecia aerate. (Bar=100 μm).

Table 1

Mouse genotype distribution.

	Scheme 1		Scheme 2	
	Genotype	**Number (%)**	**Genotype**	**Number (%)**
F2	Cre^+; wt/wt	10 (33%)	Cre^+; wt/flox	10 (26%)
	Cre^+; wt/Δ	6 (20%)	Cre^+; flox/Δ	6 (15%)
	wt/wt	4 (14%)	wt/flox	11 (28%)
	wt/Δ	10 (33%)	flox/Δ	11 (28%)
			Cre^+; wt/flox/Δ	1 (3%)
F3	wt/wt	4 (15 %)	flox/flox	16 (27%)
	wt/Δ	23 (85%)	flox/Δ	28 (48%)
	Δ/Δ	**0 (0%)**	**Δ/Δ**	**15 (25%)**